ECMWF and ERS-1 Surface Winds Over the Arabian Sea During July 1995

David Halpern

Earth and Space Sciences Division

Jet Propulsion Laboratory

California Institute of Technology

Pasadena, CA 91109

Michael H. Freilich

College of Oceanic and Atmospheric Sciences

Oregon State University

Corvallis, OR 97331

Robert A. Weller

Department of Physical Oceanography

Woods Hole Oceanographic Institution

Woods Hole, MA 02543

8 September 1998

ABSTRACT

The European Centre for Medium-Range Weather Forecasts (ECMWF) and Institut Francais Pour la Recherche et l'Exploitation de la Mer (IFREMER) European Remote-Sensing Satellite (ERS-1), named IFR2, surface wind velocity data products are compared during July 1995 over the Arabian Sea. Substantial differences were found. The central positions of the maximum isotach were separated by 450 km, and the ECMWF maximum isotach was 2 m s^{-1} higher than IFR2. IFR2 wind components contained about 10 times more variance than ECMWF winds for horizontal distances from 50 to 250 km. Along the 8.5°N southern boundary of the Arabian Sea, ECMWF southward Ekman transport was higher than IFR2 by an amount that could be observed with current measurements. The ECMWF and IFR2 difference in upward transport of water into the Ekman layer, computed from wind stress curl, was large enough to measure.

1. Introduction

Surface wind velocity data products for the Arabian Sea are available from a variety of sources: wind reports from ships; operational wind field analyses produced at numerical weather prediction (NWP) centers; and wind velocity computed from satellite scatterometer measurements. Ship reports do not have uniform error characteristics and are highly aliased in time and space. The NWP data products suffer because of incomplete parameterizations of physical and thermodynamical processes and because of sparse distribution of ship wind observations used in data assimilation. Since the July 1991 launch of the first European Remote-Sensing Satellite (ERS-1), surface wind velocity fields have been created from scatterometer data.

This paper describes a comparison between ERS-1 IFR2 (Anonymous, 1996) and European Centre for Medium-Range Forecasts (ECMWF) 10-m height wind velocity data products over the Arabian Sea for July 1995. We used the 6-hour, 1.125° x 1.125° ECMWF wind data product. The Institut Francais Pour la Recherche et l'Exploitation de la Mer (IFREMER) produced, in addition to IFR2, a version of the ECMWF wind product that was collocated with IFR2 measurements (Anonymous, 1996), which we named ECMWF/IFR. We chose July because it is

climatologically the month with highest wind speeds (Hastenrath and Lamb, 1979) and in July 1995 several international oceanographic field campaigns provide additional data.

In this report, the level of physical oceanographic significance between monthly mean wind speeds is 1 m s^{-1}. For oceanographic and meteorological conditions encountered at the IMET buoy (15.5°N, 61.5°E), where measurements of surface meteorological and upper-ocean variables had been recorded (Weller, 1996), a ± 1 m s^{-1} change in the 1-minute wind speed measured during July 1995 corresponded to a net surface heat flux of ± 8 W m^{-2}. This value is about the precision required for studies of climate variability (Bretherton, 1981).

2. Results

The patterns and general features of the July 1995 mean IFR2, ECMWF, and ECMWF/IFR wind velocities over the Arabian Sea were qualitatively similar (Figures 1). Boundaries of the Arabian Sea were arbitrarily defined to be 8.5°N, 24°N, 50°E, and 77°E. Distortions of the ECMWF/IFR isotachs compared to ECMWF (Figures 1B and 1C) were introduced by the ERS-1 scatterometer sampling scheme (Zeng and Levy, 1995).

In July 1995 the location and magnitude of the maximum isotach varied with data product (Figure 1). For ECMWF and ECMWF/IFR, the region of maximum isotach (16 m s^{-1}) was centered at 10°N, 53°E. The ECMWF and ECMWF/IFR maximum isotach was 2 m s^{-1} greater than the IFR2 maximum isotach; the difference was twice the acceptable uncertainty. The IFR2 data had three regions enclosed with the same maximum isotach (14 m s^{-1}), with the largest area centered at 13°N, 56°E. This site was 450 km northeast of the centers of the ECMWF and ECMWF/IFR maximum isotach. Examination of Special Sensor Microwave Imager wind speeds (Wentz, 1997) showed that the position and magnitude of the maximum isotach (13 m s^{-1}) were more similar to those computed with IFR2 data compared to ECMWF data.

a. Regression analysis

For IFR2 speeds below (above) 8.7 m s^{-1}, ECMWF/IFR speeds were lower (higher) than IFR2 speeds (Figure 2). For IFR2 speeds between 3 and 14 m s^{-1}, the regression line was within 1 m s^{-1} of the 1:1 line of perfect correspondence. For IFR2 speeds greater than 15 m s^{-1}, the predicted residual speed between ECMWF/IFR and IFR2 was greater than 1 m s^{-1}. The correlation coefficient between ECMWF/IFR and IFR2 wind speeds was 0.8, which was significant at the 95% confidence level. In this report, the level of statistical significance is 95%. Large differences between collocated ECMWF/IFR and IFR2 speeds yielded a rms difference of 2.1 m s^{-1}, which was twice the desired level of uncertainty.

b. Temporal variability

The July 1995 ECMWF/IFR and IFR2 1° x 1° wind speed variances averaged over the Arabian Sea were 4.8 and 3.6 m^2 s^{-2}, respectively, which were significantly different, according to the *F*-test. To examine the representativeness of the ECMWF temporal structure, 6-hour ECMWF and IMET data were compared for July 1995. IMET data were averaged over 6 hours centered on the ECMWF forecast time. The ECMWF and IMET July 1995 mean wind speed difference was less than 1 m s^{-1}. However, the ECMWF u variance (3.3 m^2 s^{-2}) and v variance (4.1 m^2 s^{-2}) were nearly two and three times, respectively, greater than the corresponding IMET variances. The differences between the ECMWF and IFR2 wind component variances were significant.

Spectra of ECMWF and IFR2 u and v components yielded the distribution of variance with frequency (Figure 3). In contrast to the large difference in IMET u spectral levels between low and high frequencies, the ECMWF u spectrum was almost flat. At the diurnal frequency and at higher frequencies, the ECMWF u spectral values were significantly different. Significant statistical difference of spectral estimates means that confidence intervals associated with ECMWF and IFR2 spectral values at the same frequency did not overlap. In the ECMWF v component, the amplitude of the diurnal-period oscillation was significant. At the diurnal period, the ECMWF rms wind speed amplitude (0.8 m s^{-1}) was 2.7 times greater than that computed with IMET data.

We did not expect ECMWF data to have more temporal variability than IMET data. In the ECMWF forecast-analysis system, data gaps of the surface wind field to be ingested into the atmosphere model were filled with previous forecasts, which should reduce temporal variability.

c. Spatial variability

The IFR2 data occurred along 19 cell tracks parallel to the ERS-1 ground track. During July 1995, there were 102 cell tracks, each with 72 25-km elements, in the region bounded by 56°E - 70°E along 8°N and by 60°E - 68°E along 24°N. The 6-hour ECMWF data between 8 and 24°N were interpolated to 72 24.4-km intervals along five meridians (61, 62, 63, 64 and 65°E). Before computing the periodogram, the u- and v-components along each cell track (for IFR2) and meridian (for ECMWF) were prewhitened to reduce spectral leakage. For IFR2, the spectral estimate for each wave number k_i was equal to the arithmetic mean value of the 102 recolored periodogram ordinates at k_i. For ECMWF, spectral estimates were computed from 124 periodograms along each meridian, and then the 5-meridian average spectra were computed. For ECMWF spectra, confidence limits are not easily determined because each 6-hour wind field was not an independent representation of the wind field. We arbitrarily allow the ECMWF-spectral confidence intervals to equal that corresponding to 204 degrees of freedom, instead of 1240 degrees of freedom had each ECMWF wind field been independent.

For wave lengths smaller than 400 km, IFR2 u- and v-spectral estimates were significantly larger than ECMWF, with differences increasing from one-third at 400 km to nearly one-hundred at 50 km (Figure 4). Stoffelen (1997) reported that ERS-1 winds, which had been computed with an algorithm different than the one we used, contained substantially more variance than ECMWF winds on scales between 50 and 250 km. It is not surprising that ECMWF data have lower variability in space compared to IFR2 because the ECMWF assimilation scheme used a weighted average of all data less than 3 hours apart from the 6-hour forecast verification time and over a 500 km region. This is in marked contrast to the instantaneity and 50-km resolution of IFR2 data.

The ECMWF u- and v-spectra displayed significant peaks of approximately equal amplitude at 64 km; the IFR2 spectra contained no such spectral peak (Figure 4). The variance at 64 km was 10^4 times smaller than that at 1000 km. No hypothesis nor previous observation justify a spectral peak at 64 km, indicating that the small-amplitude spectral peak is spurious.

Throughout the 1800- to 50-km range, the IFR2 u- and v-spectral (log-log) slopes were -2.6 and -2.4, respectively (Figure 4), which were nearly 25% greater than those computed by Freilich and Chelton (1986) for the tradewind zone in the Pacific Ocean.

d. Wind-driven ocean transports

Employing conservation of mass, a lowest-order approximation of Arabian Sea southwest monsoon wind-driven ocean circulation is meridional flow across the southern boundary at 8.5°N, vertical exchange between the thermocline and near-surface layers, and water entering the Arabian Sea by the narrow Somali Current. Attention is focused on Ekman transport and upward transport into the near-surface layer, which were computed by methods described in Halpern et al. (1998).

Along the Arabian Sea southern boundary at 8.5°N, the integrated southward Ekman transports in July 1995 for ECMWF, ECMWF/IFR, and IFR2 were -17.5, -16.7, and -12.5 Sv (1 Sverdrup (Sv) = $1x10^6$ m^3 s^{-1}), respectively. The 4.2 Sv difference between ECMWF/IFR and IFR2 would correspond to a southward Ekman current averaged over 50 m of 3 cm s^{-1}, which is a measurable quantity.

The July 1995 ECMWF, ECMWF/IFR, and IFR2 vertical transports into the Ekman layer integrated over the Arabian Sea north of 8°N were 6.3, 5.2, and 3.2 Sv, respectively. The 2 Sv (or 48%) difference between ECMWF/IFR and IFR2 corresponded to an average vertical velocity uncertainty of $0.6x10^{-6}$ m s^{-1}. This value is comparable to the error associated with vertical velocity estimated from the continuity equation and horizontal current measurements. North of 13°N where vertical motion was upward, the average difference between ECMWF/IFR and IFR2 vertical velocities was $1.8x10^{-6}$ m s^{-1} or three times greater than the average over the Arabian Sea.

4. Concluding Remarks

Results included: (1) ECMWF/IFR wind speeds were greater (smaller) than IFR2 at high (low) wind speeds; (2) IFR2 maximum isotach (14 m s^{-1}) was centered 450 km towards the northeast and was 2 m s^{-1} smaller compared to ECMWF maximum isotach (wind speed differences greater than 1 m s^{-1} were significant); (3) at all frequencies ($1.34x10^{-3}$ - $8.33x10^{-2}$ cycles per hour) ECMWF wind component spectral values were greater than those computed from moored-buoy wind observations at 15.5°N, 61.5°E, and at the diurnal period the ECMWF wind speed amplitude was nearly three times greater than that computed with wind recorder data; (4) zonal and meridional spectral values of ECMWF motions were significantly smaller than IFR2 for horizontal scales from 400 - 50 km; (5) IFR2 southward Ekman transport integrated along 8.5°N was substantially greater than that computed with ECMWF data; and (6) upward transport of water into the Ekman layer over the Arabian Sea was less for IFR2 than ECMWF, especially over the northern Arabian Sea.

Studies of wind-driven ocean circulation, especially those related to monsoon dynamics of the Arabian Sea, require accurate winds. Local wind-driven velocities, away from the coast, are essentially linearly related, at each frequency, to the wind stress (Weller, 1981), and the higher ECMWF energy levels (Figure 3) would result in stronger wind-driven currents and shear at the base of the mixed layer compared to IFR2. ECMWF southward Ekman transport and upward transport into the Ekman layer would yield stronger meridional overturning circulation in the North Indian Ocean compared to IFR2. Further studies are warranted with other NWP wind products, as well as numerical simulations utilizing these products.

Acknowledgements. We are extremely grateful to the IFREMER Centre ERS d'Archivage et de Traitement (CERSAT) for producing and distributing ECMWF/IFR and IFR2 data. Dr. Frank Wentz (Remote Sensing Systems) kindly provided SSMI winds for July 1995. The manuscript benefited greatly from constructive comments by Dr. Craig Lee (WHOI), Dr. Ad Stoffelen (KNMI), and two anonymous reviewers. Data processing and graphics were made by Peter Woiceshyn (JPL) in his usual proficient manner. The work described in this paper was

supported by NASA 622-47-09 (DH); NASA SeaWinds Project 229-18-41 (DH); NASA NSCAT Project via JPL contract 959351 (MHF); and ONR grant N00014-94-1-0161 (RW). The research described in this paper was performed, in part, by the Jet Propulsion Laboratory, California Institute of Technology, under contract with the National Aeronautics and Space Administration.

REFERENCES

Anonymous, 1996: Off-line wind scatterometer ERS products — User manual. CERSAT Ref. C2-MUT-W-01-IF: V2.0, Dept. Ocean. from Space, IFREMER, Plouzane (France), 85 pp.

Bretherton, F., 1981: The ocean surface energetics — A need for climate understanding. *Applications of Existing Satellite Data to the Study of the Ocean Surface Energetics*, C. Gautier, Ed., University of Wisconsin Press, Madison (Wisconsin), 5-14.

Freilich, M. H., and D. B. Chelton, 1986: Wave number spectra of Pacific winds measured by the Seasat scatterometer. *J. Phys. Oceanogr.*, **16**, 741-757.

Halpern, D., M. H. Freilich, and R. A. Weller, 1998: Arabian Sea surface winds and ocean transports determined from ERS-1 scatterometer. *J. Geophys. Res.*, in press.

Hastenrath, S., and P. J. Lamb, 1979: Climatic Atlas of the Indian Ocean. University of Wisconsin Press, Madison, Madison. [ISBN 0-299-07814-0]

Stoffelen, A., 1997: Towards the true near surface wind speed: Error modeling and calibration using triple collocation. *J. Geophys. Res.*, in press.

Wentz, F. J., 1997: A well-calibrated ocean algorithm for special sensor microwave/imager. *J. Geophys. Res.*, **102**, 8703-8718.

Weller, R. A., 1996: In situ observations of surface meteorology and air-sea fluxes. 1996 U.S. WOCE Report, Dept. Ocean., Texas A&M University, College Station (Texas), 17-20.

Weller, R. A., 1981: Observations of the velocity response to wind forcing in the upper ocean. *J. Geophys. Res.*, **86**, 1969-1977.

Zeng, L., and G. Levy, 1995: Space and time aliasing structure in monthly mean polar-orbiting satellite data. *J. Geophys. Res.*, **100**, 5133-5142.

List of Figures

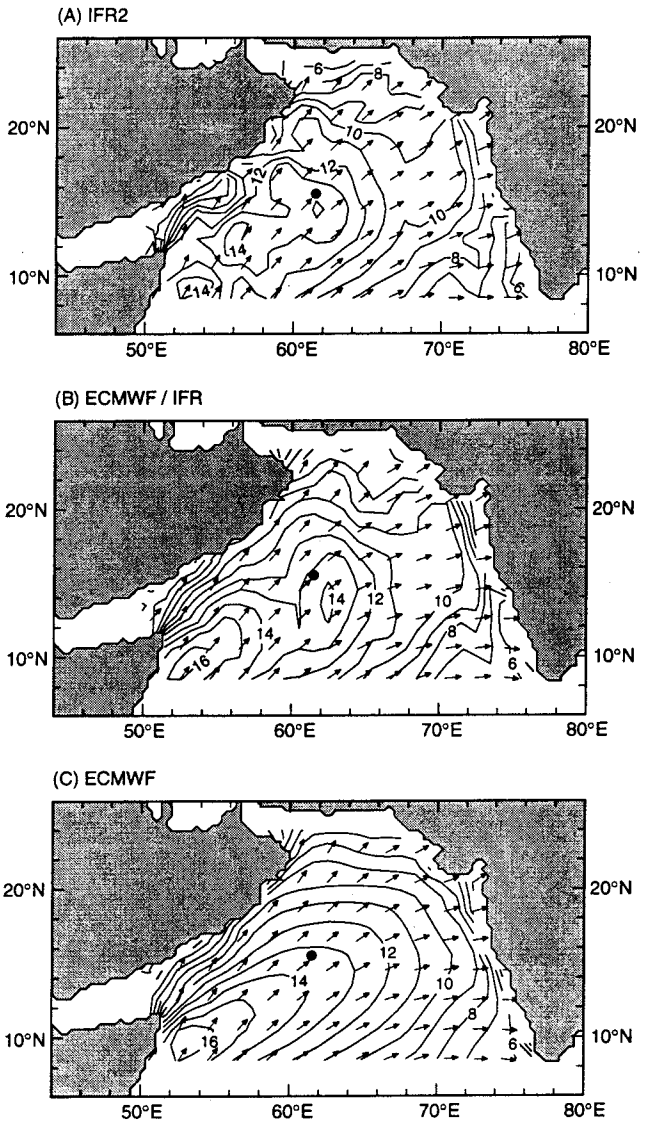

Figure 1

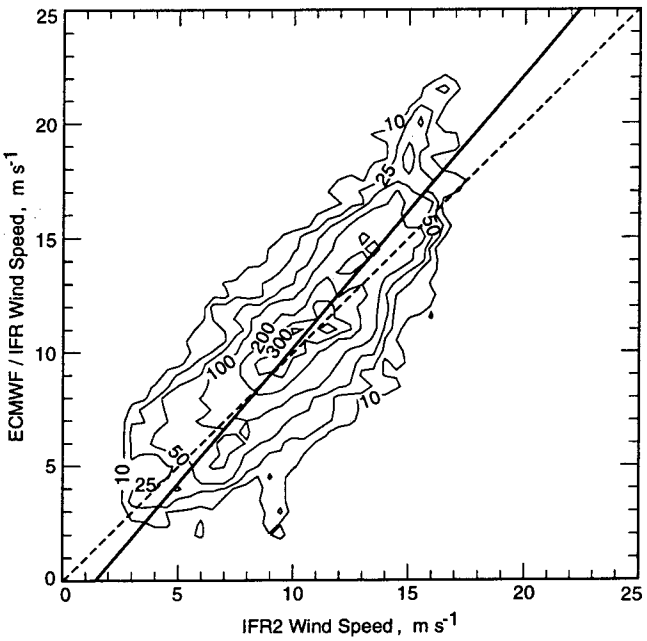
ECMWF / IFR Wind Speed, m s-1
IFR2 Wind Speed, m s-1
0
5
10
15
20
25
10
25
50
100
200
300
10
25
50
10

Figure 2

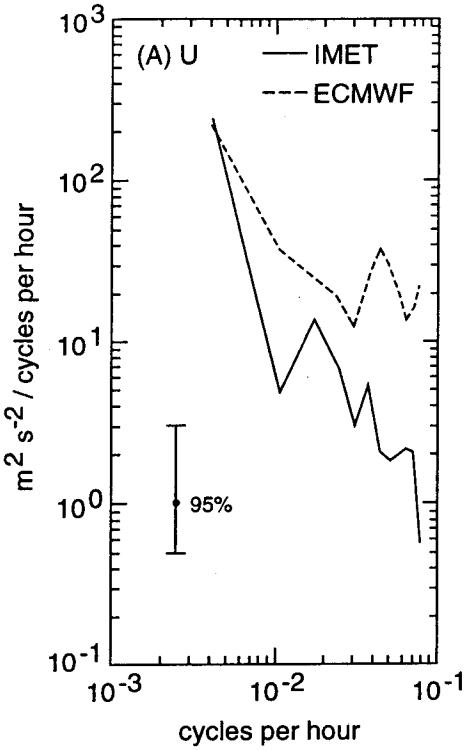
(A) U
IMET
ECMWF
95%
10^3
10^2
10^1
10^0
10^{-1}
10^{-3}
10^{-2}
10^{-1}
$m^2\ s^{-2}$ / cycles per hour
cycles per hour

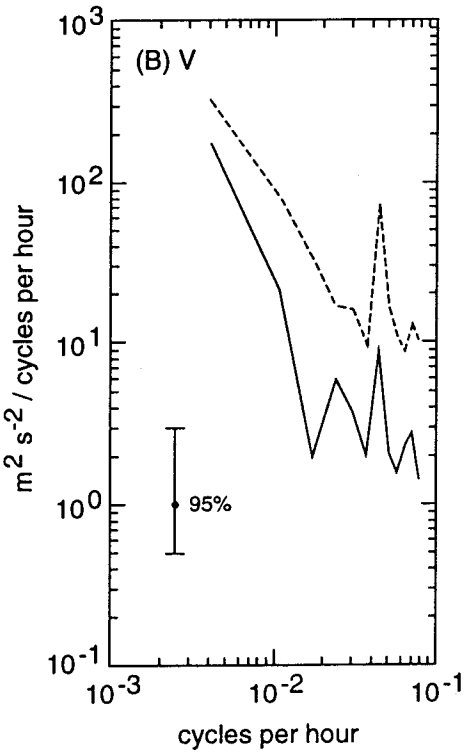
(B) V
95%
10^3
10^2
10^1
10^0
10^{-1}
10^{-3}
10^{-2}
10^{-1}
$m^2\ s^{-2}$ / cycles per hour
cycles per hour

Figure 3

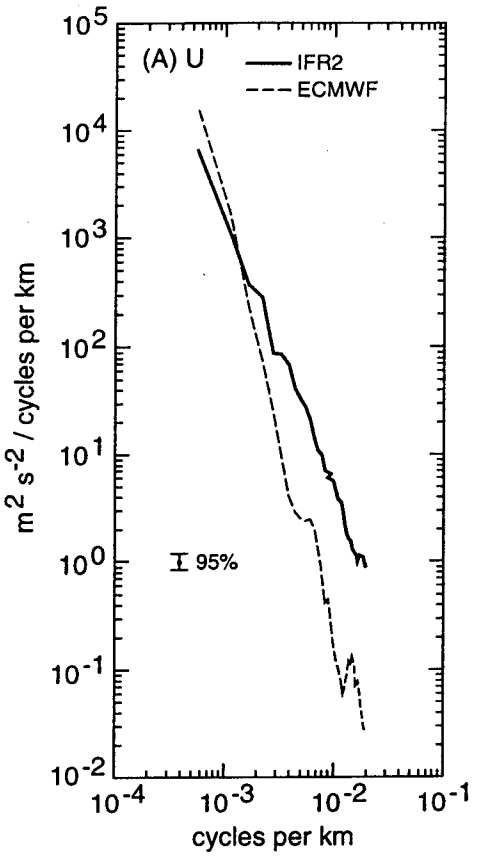
(A) U
IFR2
ECMWF
95%
$m^2\ s^{-2}$ / cycles per km
cycles per km
10^5
10^4
10^3
10^2
10^1
10^0
10^{-1}
10^{-2}
10^{-4}
10^{-3}
10^{-2}
10^{-1}

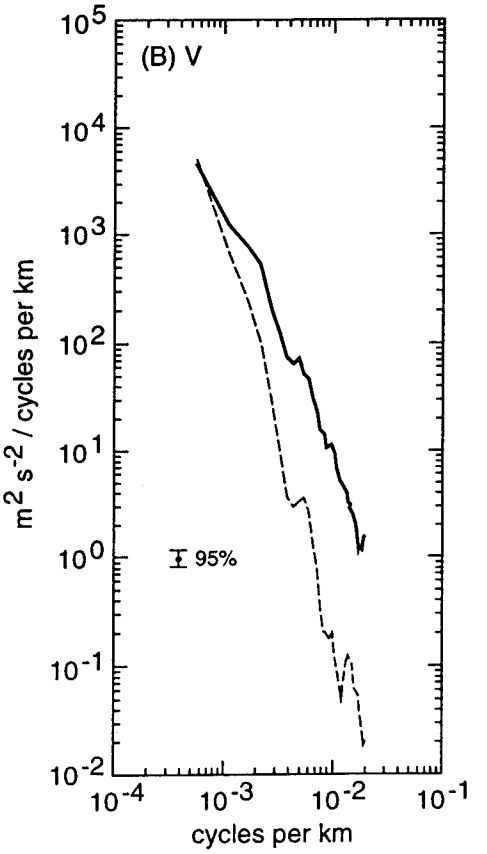
(B) V
95%
$m^2\ s^{-2}$ / cycles per km
cycles per km
10^5
10^4
10^3
10^2
10^1
10^0
10^{-1}
10^{-2}
10^{-4}
10^{-3}
10^{-2}
10^{-1}

Figure 4